

Enthalpic effects on interfacial adhesion of immiscible polymers compatibilized with block copolymers

A. Adedeji and A. M. Jamieson*

Department of Macromolecular Science, Case Western Reserve University, Cleveland, OH 44106, USA

(Received 8 March 1993)

The influence of enthalpic interactions on interfacial adhesion between immiscible polymer matrices and reinforcing block copolymer segments has been studied using the transmission electron microscopic (TEM) methodology of Creton *et al.* We examined the behaviour of four statistical styrene-acrylonitrile (SAN) copolymers, each having different acrylonitrile (AN) content, blended with polystyrene (PS) as the minor component, and reinforced by three poly(methyl methacrylate-*b*-styrene) (PMMA-*b*-PS) block copolymers of differing molar masses, viz. 20 000, 65 000 and 680 000 g mol⁻¹. These observations were compared with similar experiments on poly(methyl methacrylate) (PMMA) blended with PS and reinforced by PMMA-*b*-PS. Emulsification was observed with all three PMMA-*b*-PS copolymers. Crazes were formed in the SAN matrices and a statistical evaluation of interfacial failures was performed on the discrete PS domains that lay within the crazes. For the two block copolymers of higher molar mass, optimal reinforcement of the interfaces was observed independent of the SAN composition. With the 20 000 block copolymer, however, the pattern of the interfacial failure depended strongly on the SAN composition. Specifically, it was observed that the fraction of the discrete particles that suffered interfacial failure, and led to the creation of large voids in the crazes in these blends, increased with increased AN content of the SAN matrix. Thus, we found that the fraction of discrete PS particles that produce large voids in crazes of blends containing SAN33 is always higher than in blends containing SAN15, when reinforced with the 20 000 PMMA-*b*-PS. We infer that the critical molar mass required of a mechanically reinforcing copolymer depends on the short-range (attractive and repulsive) interactions between the blend components in the interfacial region. The TEM method could not, however, distinguish between reinforced and neat PMMA/PS blends, all of which showed strong adhesion. This is attributed to the comparatively diffuse interface in the PMMA/PS system, a consequence of the relatively weak repulsion between these two polymers.

(Keywords: immiscible blends; interfacial adhesion; enthalpy)

BACKGROUND

Pairs of immiscible polymers form narrow interfaces between the two separated phases as a result of comparatively high interfacial tension^{1,2}. The interfacial tension increases and the interfacial width decreases with higher degree of incompatibility of the components A and B. Thus, a mean-field theoretical description yields the following results³:

$$\gamma \sim (\chi_{AB})^{1/2} \rho_0 kT$$

and

$$d/b \sim (\chi_{AB})^{-1/2}$$

where γ is the interfacial tension, d is the interfacial width, ρ_0 is the number-average density, b is the Kuhn statistical length, k is Boltzmann's constant, T is absolute temperature and the Flory-Huggins interaction parameter, χ_{AB} , is a positive constant describing the endothermic interaction between the two components. The interfacial tension in such a blend can be lowered by adding a block copolymer (A-*b*-B) whose segments are chemically identical to the dissimilar polymers and which preferentially localizes at

the interface. We refer to this as an A/A-*b*-B/B blend. A similar effect can be obtained when one adds a block copolymer whose block segments are chemically dissimilar to the matrix components, but which exhibits an exothermic interaction with only one of the blend components (e.g. an A/X-*b*-Y/B blend with $\chi_{AX} < 0$, $\chi_{BY} < 0$, $\chi_{AY} > 0$, $\chi_{BX} > 0$, $\chi_{XY} > 0$). The lowering of interfacial tension leads to a decrease in size of the disperse phase domains, i.e. an emulsification effect.

The overall mechanical response of blends of immiscible polymers depends on the mechanical properties of the component polymers, on the blend morphology and on the degree of mechanical contact between the phases. Incompatible binary blends (A/B) generally show poor mechanical strength owing to the comparatively high interfacial tension, which leads to a narrow interface and poor adhesion, resulting in easy de-wetting of the phases during mechanical loading. This results in fracture of the blend at low strains and stresses, which clearly limits the utility of such mixtures⁴. Addition of an emulsifying block copolymer can result in an enhancement of the interfacial adhesion (mechanical compatibilization) if each block can selectively mix with blend components.

* To whom correspondence should be addressed

This interfacial adhesion enhancement indicates a mechanical coupling between the block copolymer segments and the respective homopolymers⁵. Indeed, such improvement in mechanical integrity of A/A-*b*-B/B or A/X-*b*-Y/B polymer-polymer mixtures has been attributed to the formation of entanglements between the diblock copolymer segments and the matrices on both sides of the interface, which effectively function as 'hooks' between the two phases⁵. The added third component A-*b*-B or X-*b*-Y thus leads to a better stress transfer between the phases^{4,6}.

The utility of block copolymers in compatibilizing immiscible polymers is well established. However, a brief discussion of previous studies of mechanical compatibilization seems appropriate. An extensive review on interfacially active agents for immiscible polymer blend systems has been given, covering the years between 1982 and 1987, by Xanthos⁷. Various theoretical models have been developed to describe the molecular mechanisms of emulsification and compatibilization by block copolymers⁸⁻¹⁴. The basic physics of the emulsification process involves localization of the copolymer A-*b*-B or X-*b*-Y at the interface between A and B, which leads to a loss of configurational entropy. However, this loss is compensated by a gain in enthalpy due to the placement of the compatible blocks in the appropriate homopolymer phases, such that the overall interfacial free energy is lowered^{9,10}. A particular theoretical analysis, by Noolandi and Hong^{9,10}, of interfacial tension in the A/A-*b*-B/B system showed, in agreement with other independent analyses¹²⁻¹⁴, that the interfacial tension decreases as block copolymer molar mass and the interaction parameter χ_{AB} increase. A subsequently generalized theory of interfacial tension in the A/X-Y/B system^{15,16} yielded expressions for the interfacial tension and the width of the interface as a function of the various χ parameters, χ_{AX} , χ_{XY} , χ_{YB} , etc. (where all the interaction parameters are endothermic). Thus, for the A/X-*b*-Y/B system when $\chi_{AY} > \chi_{AX}$ and $\chi_{BX} > \chi_{BY}$, locally, there will be a thermodynamic driving force to orient the block copolymer at the interface, thus leading to a wider interface and lower interfacial tension.

Barlow and Paul⁴ have experimentally related improvement in mechanical properties, particularly ductility, for a variety of immiscible binary blends to the degree of adhesion developed between the phases by incorporating compatibilizers (block and graft copolymers). The compatibilizers utilized were of high molar mass, particularly for an ethylene-propylene-ethylidene norbornene copolymer that was used to reinforce low-density polyethylene (LDPE) and polypropylene (PP), and which had an ethylene segment that was long enough to show ethylene crystallinity. Brown¹⁷ examined the dependence of interfacial toughness on the amount and molar mass of added copolymer using a model polystyrene/poly(methyl methacrylate) (PS/PMMA) system containing approximately symmetrical PS-*b*-PMMA block copolymers with molar masses ranging from 84 000 to 900 000 g mol⁻¹. It was observed that the presence of block copolymer can increase toughness by a factor as high as 50 and that the ultimate toughness can be achieved when the block copolymer thickness is equal to one-half of the neat block copolymer long period. With regards to the origin of the mechanical reinforcement, Brown¹⁷ proposed that an increment in the interfacial width results in an increase in the

number of entanglements in the interfacial region, which is the source of the mechanically improved interfacial strength. In addition, Shull and Kramer¹³ have suggested that it is the penetration of the block copolymer segments into the homopolymer phases that controls the enhanced adhesion. Brown¹⁸ also investigated improved mechanical properties in a poly(2,6-dimethylphenylene oxide) (PPO)/PMMA immiscible blend, compatibilized with a symmetrical diblock copolymer PS-*b*-PMMA of molar mass 300 000 g mol⁻¹. Here, PS and PPO are chemically dissimilar but exhibit an exothermic interaction. It was reported¹⁹ that the PS-*b*-PMMA copolymer increased the interfacial toughness from 1.5 to 15 J m⁻². Brown *et al.*²⁰ further measured the interfacial width in the PS/PPO-*b*-PMMA/PMMA system. It was demonstrated, using secondary ion mass spectrometry (s.i.m.s.) with quadrupole mass analysis and secondary ion mass detection to measure the block copolymer depth profiles, that the PS segment of the copolymer was more swollen than the PMMA segment by at least a factor of 2. It was concluded that a small favourable enthalpy of mixing can cause significant swelling of a copolymer segment in a polymeric solvent²⁰. One might anticipate that such an increase in interfacial width would improve interfacial adhesion, but no experimental confirmation of this exists, to our knowledge.

Most of the earlier work summarized in this brief review utilized block copolymers of molar masses that are high enough to form entanglements with the two immiscible phases. Creton *et al.*⁵ demonstrated the existence of a minimum degree of polymerization necessary for good mechanical performance in an immiscible blend of polystyrene (PS) and poly(2-vinylpyridine) (PVP) compatibilized with a diblock poly(styrene-*b*-2-vinylpyridine) (PS-*b*-PVP) copolymer. A reduction in interfacial tension was observed over the entire range of block copolymer molar masses. However, a mechanical reinforcement effect was found only in cases where the molar masses of the block copolymers were greater than the average molar mass between entanglements, consistent with the idea that at least one entanglement between the block copolymer and the homopolymer matrix is necessary for strong adhesion.

The toughness of glassy polymers such as styrene-acrylonitrile (SAN), PS and PMMA has been attributed to their ability to dissipate energy, under tensile stresses, by structurally transforming their bulk structure to produce crazes. The tensile strength of glassy polymers increases appreciably with molar mass M , and approaches an asymptotic value beyond which no further increase occurs²¹. This effect has been attributed to entanglement slippage in the lower-molar-mass polymers³⁸. As the molar mass decreases below a critical value M_c , numerically comparable to the entanglement molar mass M_e , stable craze formation in these polymers is no longer possible²² and fracture strength falls essentially to zero²³. Molecules with M less than M_c do not contribute to the mechanical strength; their presence dilutes the entanglement network and weakens the polymer²⁴. It is pertinent to note that Brown⁸ has pointed out that an interface of immiscible glassy polymers, reinforced by diblock copolymer linkages, is also expected to fail by a crazing process, but that the craze growth will not be symmetrical; the craze will grow only into the material with the lower crazing stress. When a pair of immiscible

glassy polymers such as SAN and PS is compatibilized by a diblock copolymer, interfacial failure can be expected to occur by crazing, but the craze growth will, therefore, not be mechanically symmetrical^{5,8}. If SAN is the continuous phase and PS is the disperse phase, the craze will grow from the SAN matrix into the PS phase owing to the lower PS crazing stress²⁵. Interfacial failure is, hence, expected at one side of the craze. If the interface is strong enough to transfer stress across the interface, the disperse PS domains are expected to deform; however, if the interface is weak, the craze will break down, leaving the PS domains undeformed, and leading to creation of a large void, which subsequently matures to become a crack^{5,26,27}. Fibril breakdown caused by the discrete phase particles is known to lead to premature fracture in phase-separated blends that undergo crazing⁵. Creton *et al.*⁵ used this method to establish a critical molar mass for mechanical reinforcement required of the PVP block copolymer segment in the aforementioned PS/PS-*b*-PVP/PVP system.

This investigation is designed to elucidate the influence of enthalpic interaction parameters on the interfacial adhesion of a block copolymer in an immiscible blend as a function of the molar mass of the blend components. Specifically, we aimed to establish whether the minimum block copolymer molar mass required for reinforcement is a function of the enthalpic interaction. We chose to investigate these effects in an A/X-*b*-B/B system corresponding to SAN/PMMA-*b*-PS/PS, where SAN, a statistical styrene-acrylonitrile copolymer, is the major component. In the SAN/PMMA-*b*-PS/PS blend system $\chi_{\text{SAN-PS}}$ is positive, leading to a strong repulsion between the SAN matrix and the PS segment of the diblock copolymer PMMA-*b*-PS. In addition, $\chi_{\text{SAN-PMMA}}$ is negative over a range of acrylonitrile (AN) content from 9.5 to 33%^{25,28-30}, leading to an attraction between the SAN and the PMMA block. Each of these effects will thermodynamically encourage the localization of the PMMA-*b*-PS block at the interface and lead to athermal dissolution of the PS segment in the PS homopolymer, and exothermic dissolution of the PMMA in SAN. The overall result will be an increment in the interfacial width, which is a prerequisite for good emulsification and mechanical compatibilization effects. Systematic variation of the enthalpic interaction can be obtained by varying the acrylonitrile (AN) content of the SAN³¹. In an earlier study, Akiyama and Jamieson³¹ demonstrated the influence of enthalpy-driven swelling of the PMMA block copolymer segment on the morphology of SAN/PMMA-*b*-PS/PS blends. In the following investigation, the interfacial strength in these blends is evaluated by observing the deformation and fracture of polystyrene inclusions in crazes formed in thin films, following the methodology of Creton *et al.*⁵.

EXPERIMENTAL

Materials

Statistical copolymers of styrene-acrylonitrile (SAN) with acrylonitrile contents of 15, 26, 29 and 33%, designated, henceforth, as SAN15, SAN26, SAN29 and SAN33, respectively, with specified molar masses as described in Table 1, were supplied by Mitsui Toatsu Chemicals Inc. Diblock poly(methyl methacrylate-*b*-styrene) copolymers of narrow molar-mass distribution

Table 1 Characteristics of polymer blend components

Abbreviation	Acrylonitrile content (%)	M_w ($\times 10^3$)	M_w/M_n	Weight ratio (PMMA:PS)
PMMA(127K)	–	127	1.06	–
PS(17K)	–	17	1.04	–
PS(105K)	–	105	1.06	–
SAN15	15	173	2.12	–
SAN26	26	148	2.16	–
SAN29	29	141	2.23	–
SAN33	33	102	1.95	–
B(20K)	–	20.5	1.14	10 700:9800
B(65K)	–	65.5	1.06	32 500:33 000
B(680K)	–	680	1.10	220 000:460 000

with M_w of 680 000, 65 000 and 20 000 g mol⁻¹ (see Table 1 for weight ratios), designated as B(680K), B(65K) and B(20K), respectively, were obtained from Polysciences Inc., and used without further purification. Anionic standard polystyrene homopolymers with M_w of 105 000 and 17 000 g mol⁻¹, designated as PS(105K) and PS(17K), respectively, were obtained from Pressure Chemicals. Monodisperse PMMA of M_w of 127 000 g mol⁻¹ was obtained from Polysciences Inc.

Methods

Ternary blends containing 82% w/w of SAN15, SAN26, SAN29, SAN33 or PMMA(127K) with 6% w/w of B(20K), B(65K) or B(680K) and 12% w/w of PS(17K) or PS(105K) were prepared by first dissolving the components in methyl ethyl ketone (MEK) solvent at an overall concentration of 1 g/100 ml solution. Binary blends containing 88% w/w SAN or PMMA(127K) with 12% w/w of PS(105K) were similarly prepared. Films with thicknesses of about 3000–5000 Å were formed by pulling a glass slide from these solutions. The solvent was evaporated at room temperature for 5 min. The films were floated on water (stripped off the glass substrate) and picked up on ductile 3 mm (diameter) standard copper grids. Bonding of the films onto the grids was ensured by annealing in an oven, under vacuum, for 48 h at 100°C. The films attached to the grids were stretched to generate crazes, after which they were exposed to 0.5% ruthenium tetroxide (RuO₄) vapour for 30 min, to stain the PS domains. The transmission electron micrographs of the crazes were obtained on a JEOL 100-SX TEM.

RESULTS AND DISCUSSION

The electron micrographs of the blends show the discontinuous PS phase as discrete dark spherical particles, randomly dispersed in a lightly stained SAN or PMMA continuous phase. The PS domain sizes were significantly reduced on addition of PMMA-*b*-PS for all the three molecular weights of PMMA-*b*-PS, comparable to the behaviour observed by Creton *et al.*⁵ in the PS/PS-*b*-PVP/PVP system. The craze widths are typically 800 nm, being determined by the molar mass of the SAN (or PMMA)²⁶. The micrographs, shown in Figures 1a–d, of crazes in the binary system SAN/PS(105K) are typical of the crazes observed in all the uncompatibilized binary blends. It shows that the interfaces formed in such immiscible blends fail, even at low strains, leading to creation of large voids. In contrast,

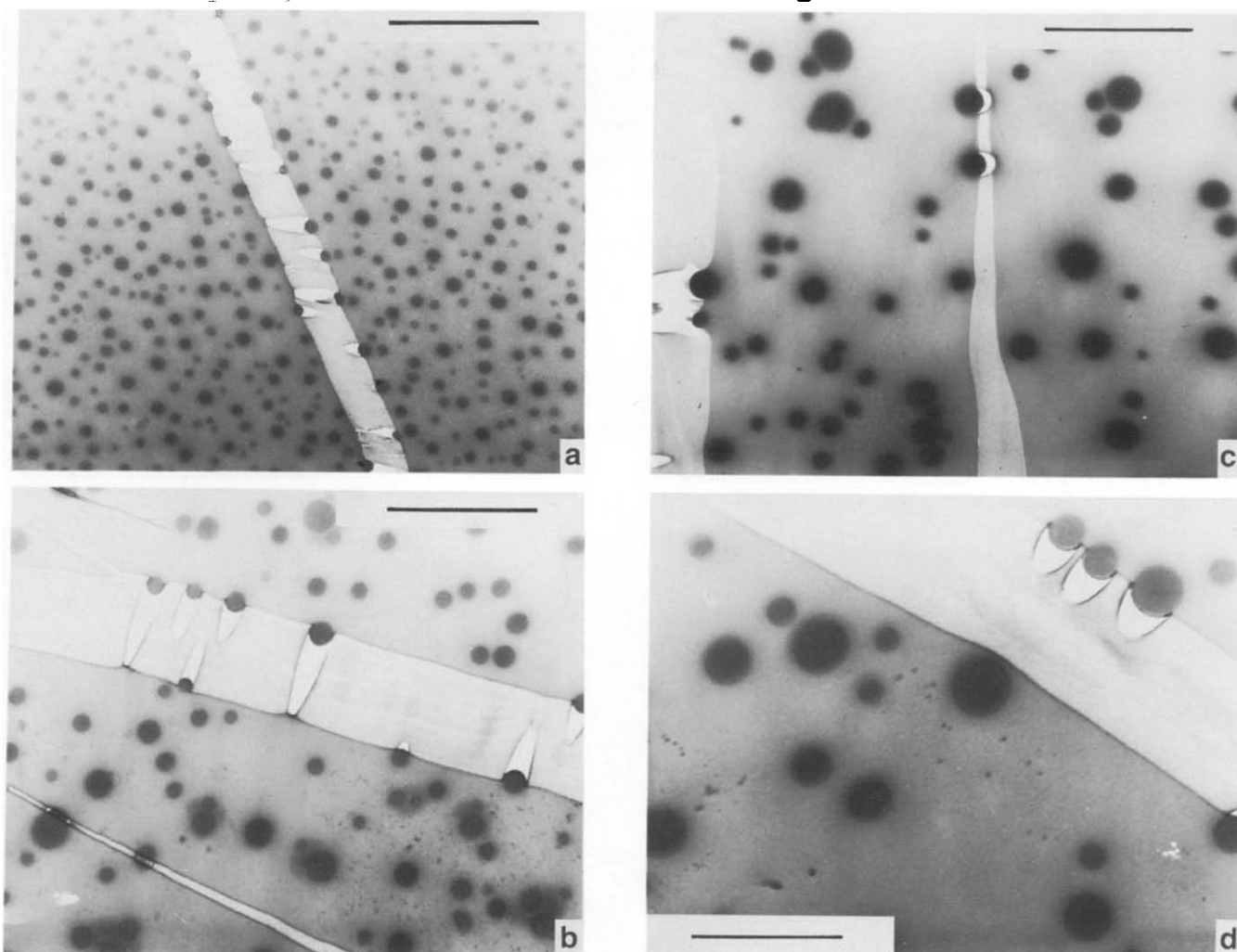


Figure 1 Undeformed PS domains in SAN/PS(105K) blends indicating weak interfaces, even at low strains as in SAN29 where failure occurs at the craze tip: (a) SAN15, (b) SAN26, (c) SAN29 and (d) SAN33. The scale bar in each case is 5 μm

micrographs of the SAN/B(65K)/PS(105K) (Figures 2a–d) and SAN33/B(680K)/PS(105K) (see Figure 3) show that the discrete PS domains are deformed from spheres to ellipsoids. Such behaviour was observed in all the ternary blends of SANs and PS(105K) compatibilized by B(65K) and B(680K), since the molar masses of each segment are well above the critical molar mass for good adhesion.

By contrast, Figures 4a–d are micrographs of crazes in the SAN/B(20K)/PS(17K) blend and indicate that, for all blends with a PS(17K) minor phase, the interfacial strength is higher than that of the homopolystyrene phase, as is clearly indicated by the broken spherical PS inclusions within the crazes. These domains fractured because the molar mass of the PS homopolymer ($17\,000\text{ g mol}^{-1}$) is below that required to sustain crazes. Thus, for all SAN species there is a stronger adhesion between the block copolymer and the SAN matrix compared to the weak cohesion between the PS(17K) and PS(17K). Finally, the crazes in the ternary blends, containing a high-molar-mass PS(105K), compatibilized with B(20K), show both fully deformed and undeformed PS spheres, as illustrated by typical crazes in the SAN/B(20K)/PS(105K) blends shown in Figures 5a–d. Visual examination indicates that the relative amount of the undeformed spheres is higher in blends containing

SANs of higher AN content. A statistical analysis (described below) was performed to estimate the average fraction of the undeformed PS spheres in each of these ternary blends.

Micrographs of crazes generated in the SAN/B(20K)/PS(105K) ternary blends in which PS is the minor component were used to evaluate statistically the effect of the adhesive strength of the block copolymer at the PS/SAN interfaces of different levels of enthalpic interaction. As illustrated schematically in Figure 6, the evaluation excluded polystyrene domains within the craze tips as well as those in any crazes whose trunks were significantly narrower than the average width of 800 nm. Particles that fell within the crazes were classified based on their diameters (nm). The fraction, f , of particles of any diameter range whose interfaces failed, leading to creation of large voids, was determined by visual examination. Fully deformed particles were counted as 0, partially deformed and undeformed particles were counted as 1 when they led to creation of voids. No significant systematic variation in f with domain particle size was observed in our experiments. Figure 7 shows the graphical representation of the f values, averaged over all domain sizes, obtained with different AN contents. The value of f shows an increase with increase in AN

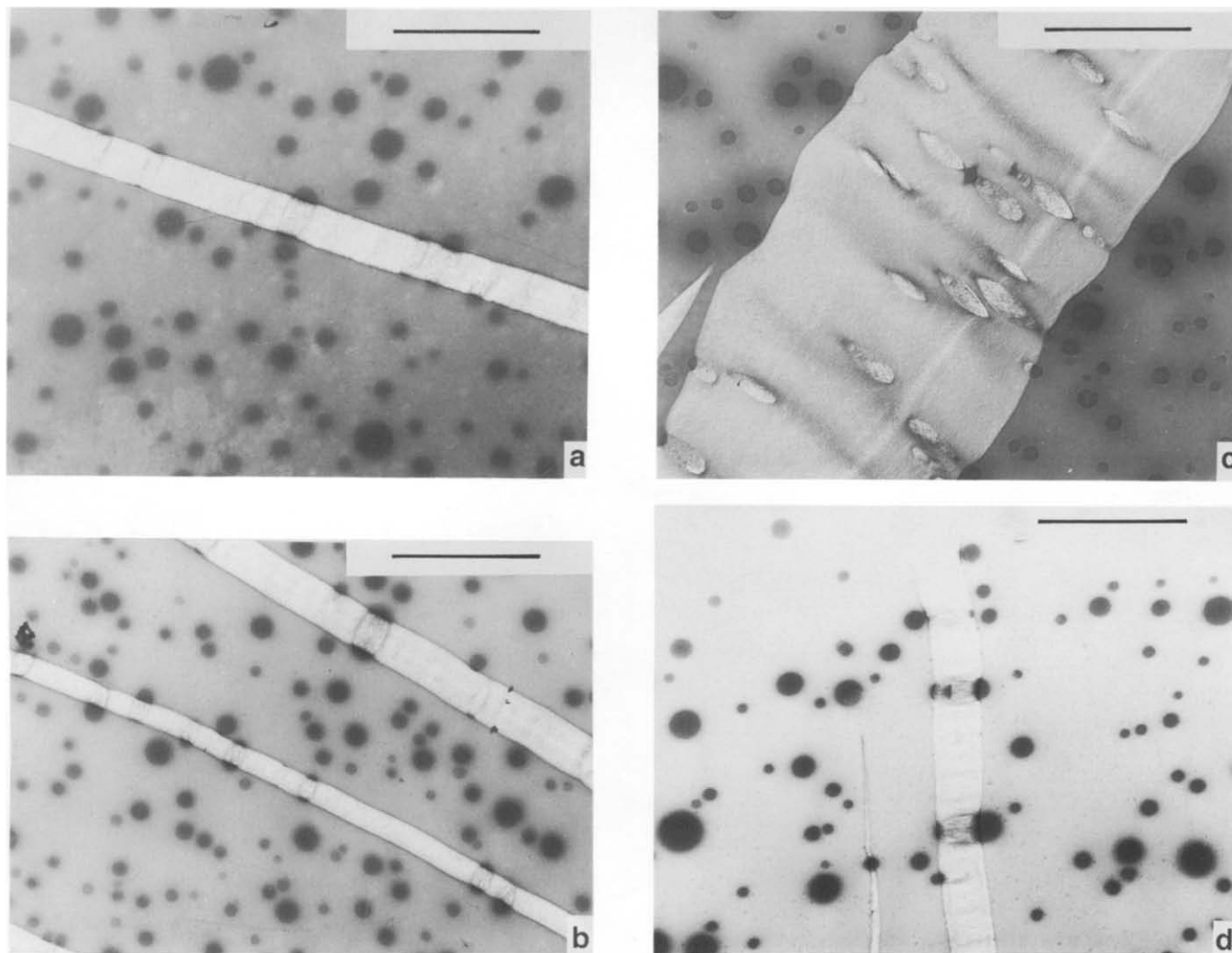


Figure 2 Deformed PS domains in SAN/B(65K)/PS(105K) blends, even at large strains as in SAN29 where fully deformed domains are evident within a large craze: (a) SAN15, (b) SAN26, (c) SAN29 and (d) SAN33. The scale bar in each case is 5 μm

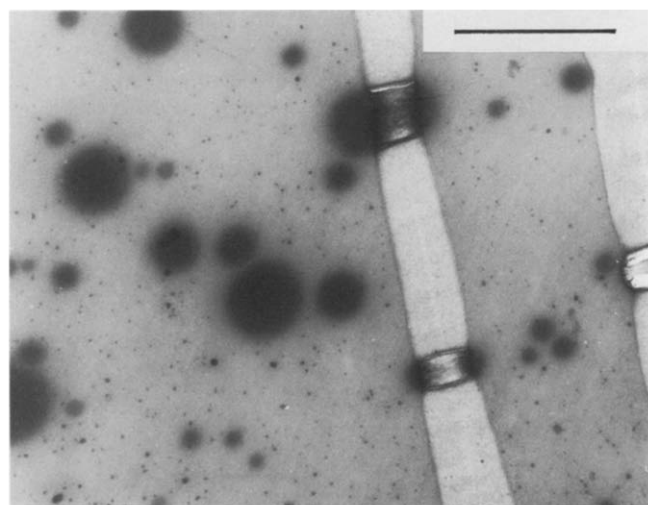


Figure 3 Deformed PS domains in SAN33/B(680K)/PS(105K) blend. Scale bar is 5 μm

content, indicating that the interfacial strength decreases with a decrease in the exothermic interaction in the PMMA/SAN.

Note that there is comparatively poor contrast in micrographs of SAN15/B(20K)/PS(105K) since SAN15 is

stained quite effectively by RuO_4 . Therefore, longer exposure times were used during the development of the positive images of these micrographs with the intention of improving the contrast within the crazes. The PS particles in this blend system are small (210–280 nm) and narrowly distributed in sizes, and often there are undeformed and partially deformed PS domains within crazes that do not create voids and are not visible in under-exposed films. Also, as explained by Creton *et al.*⁵, if the particles are very small, the voids produced may not be larger than the craze fibrils, and the craze will simply bypass the particle interfaces, and continue to draw more material from the active zone into the craze once the undeformed particles have been incorporated into the craze. Therefore, we counted the domains that created voids and those undeformed ones that did not create voids as 1. The undeformed domains that did not create voids were pessimistically rated as failures because their interfaces have been bypassed. The points plotted in Figure 7 are the mean and standard deviations of three independent experiments for SAN15 and SAN33 blends, and two experiments for SAN26 and SAN29.

Figure 8 is a composite plot of the variation in f values, again averaged over all domain sizes, when different PMMA block lengths are used to compatibilize blends of varying degrees of exothermic interaction. For

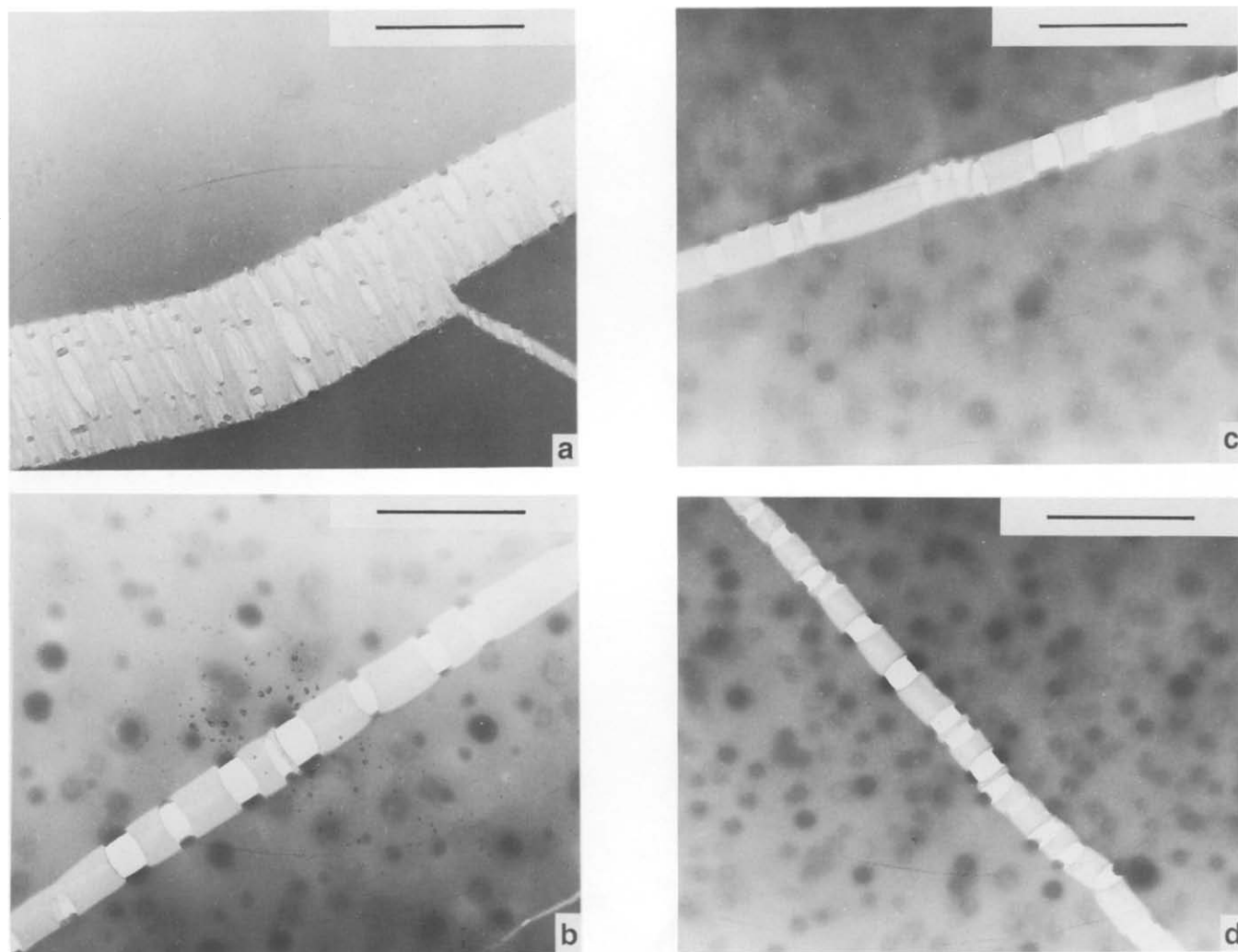


Figure 4 Broken PS spherical domains in SAN/B(20K)/PS(17K) blends: (a) SAN15, (b) SAN26, (c) SAN29 and (d) SAN33. The scale bar in each case is 5 μm

comparison, we plot data taken from the previous work of Creton *et al.*⁵ on PS/PS-*b*-PVP/PVP blends.

Our observations, summarized in *Figure 8*, suggest that the critical molar mass for strong adhesion in the SAN/PMMA-*b*-PS/PS systems is smaller than that in the PS/PS-*b*-PVP/PVP system. This is perhaps not surprising since the molar mass of the PMMA block in the B(20K) copolymer is comparable to the entanglement molar mass for PMMA ($M_e(\text{PMMA}) \sim 5000\text{--}10\,000 \text{ g mol}^{-1}$ (ref. 32)), which is smaller than that for PS ($M_e(\text{PS}) \sim 17\,000 \text{ g mol}^{-1}$ (ref. 32)). Note that the molar mass of the PS block is substantially smaller than $M_e(\text{PS})$. *Figure 7* further indicates that more particle interfaces fail in blends of higher AN content when this PS-*b*-PMMA block copolymer is used. From *Figure 8* we are led to deduce, therefore, that the critical block copolymer molar mass required for mechanical reinforcement of the interfaces is lowest in the SAN15/PS blends and systematically increases for the SANs of higher AN content. We interpret this effect as due to the more exothermic enthalpic interaction in the SAN15 blend, which increases the interfacial width. Unfortunately, we do not have available block copolymers of intermediate molar masses to obtain a more detailed picture of the crossover from strong to weak adhesion.

Finally, in *Figures 9a* and *9b*, we show typical crazes,

respectively, in the neat PMMA(127K)/PS(105K) blend and in the ternary system PMMA(127K)/B(20K)/PS(105K). No differences can be seen, presumably because of the comparatively weak PMMA-PS repulsion ($\chi_{\text{PMMA-PS}} = 0.03\text{--}0.04$ (ref. 17)). This leads to a relatively diffuse interface and good mechanical interfacial strength of the neat PMMA/PS(105K) as well as of the PMMA/B(20K)/PS(105K) blends.

Interfacial adhesion in SAN/PMMA-*b*-PS/PS blends may be influenced by three distinct types of enthalpic interaction: a weak repulsion between the two block copolymer segments, a strong repulsion between the PS block and the SAN matrix, and a smaller attractive interaction of the PMMA with the SAN matrix. The interaction energies listed on *Table 2* show that there is exothermic mixing between the SANs and the PMMA block segment, which is largest for SAN26 and smallest for SAN33; conversely, the positive interaction energies between the SANs and the PS block, two orders of magnitude higher than that of SAN-PMMA, lead to a strong repulsion of the PS block by the SAN matrix across the interface.

In addition, the entropic interaction between the block segments and the matrices must be considered, particularly when the block molar masses are higher than those of the matrix components³¹. All these

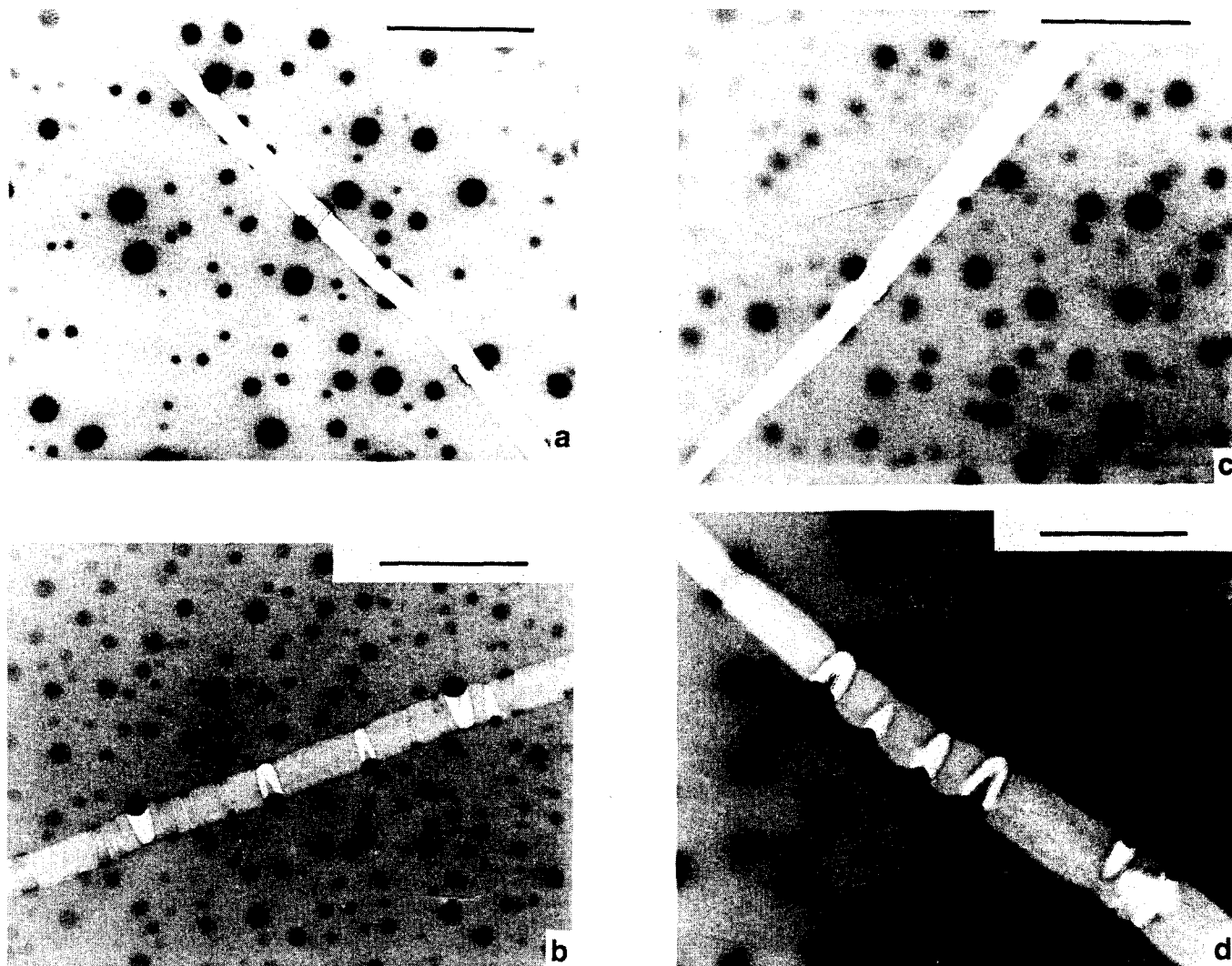


Figure 5 Crazes in SAN/B(20K)/PS(105K) blends: (a) SAN15, (b) SAN26, (c) SAN29 and (d) SAN33. The scale bar in each case is 5 μm

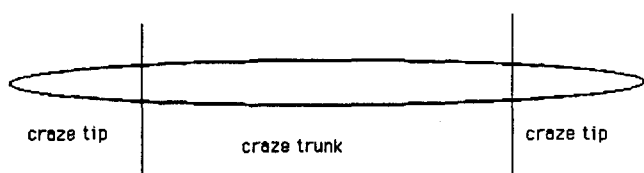


Figure 6 Schematic representation of the craze trunk that was considered for statistical analysis of failed PS particles

contributions (attractive, repulsive and entropic) can influence penetration of the block copolymer into the matrix and hence can modify the net interfacial adhesion. Therefore, we need to distinguish between the roles played by the enthalpic and the entropic effects in order to discern the trend by which enthalpy influences the interfacial adhesion. In addition, we note that reinforcement with block copolymers of molar masses lower than the critical value eliminates the possibility of having mechanical entanglements between the block segments and the matrix⁵, and results in a large decrease in intermolecular strength^{22,23}. Thus, we expect that highest sensitivity to enthalpy-driven changes in interfacial strength will be obtained with block copolymers whose segment molar masses are comparable to the corresponding entanglement molar masses.

We conclude with a consideration of the relative

contributions of these competing factors in the various blend systems included in our study.

SAN/PS(105K)

These binary blends show sharp interfaces at all four SAN compositions, which easily de-wet on deformation owing to the large positive (endothermic) interaction between each SAN and PS.

SAN/B(680K)/PS(105K)

The B(680K) block copolymer has PS(460K) and PMMA(220K) segments. These respective molar masses are each high enough for numerous entanglement couplings between the blocks and the matrices. Entropy-driven swelling of the PS(460K) and PMMA(220K) segments by the lower-molar-mass polymeric PS(105K) and SAN matrices is expected, as noted by Akiyama and Jamieson³¹, based on the extensive studies of Thomas and coworkers^{33,34}. Hence, entropic and enthalpic effects each act to increase the interfacial width and enhance the entanglement interaction across the interface, ensuring that all the SANs exhibit strong interfacial adhesion, as evidenced by the deformed PS(105K) spherical domains in Figure 3.

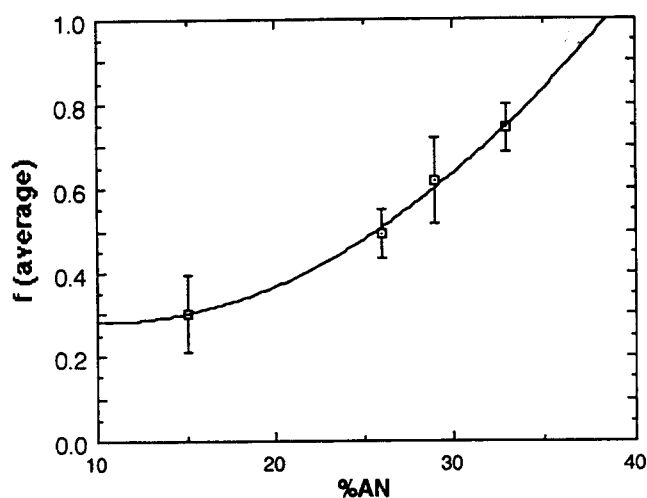


Figure 7 Average fraction of the failed PS particles within the crazes, plotted against the acrylonitrile content of the SAN matrix. Note that the data for SAN15 and SAN33 are the means of three independent experiments while those of SAN26 and SAN29 are averages of two independent experiments

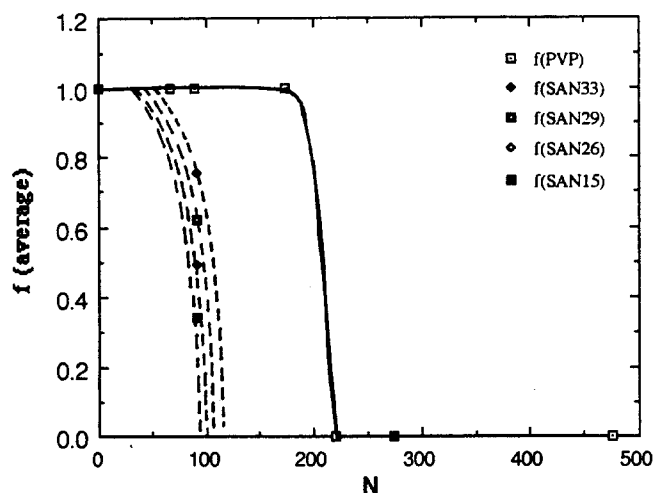


Figure 8 The fraction of interfacial failure, f , plotted against block copolymer segment length; also shown are data of Creton *et al.*⁵ on PS/PS-*b*-PVP/PVP blends

SAN/B(65K)/PS(105K)

The B(65K) block copolymer has PS(33K) and PMMA(32K) segments. These respective molar masses are each higher than that required for mechanical entanglements. However, entropy-driven swelling of the blocks is not expected to contribute to any observed increase of the interfacial width because the block molar masses are much lower than those of the matrix polymers^{31,34}. The adhesion between the SAN and the PMMA(32K) block will be enhanced by the exothermic mixing, which promotes intermolecular attraction and entanglements. Since we observed good adhesion at all SAN compositions, we deduce that the favourable enthalpic interactions, coupled to a sufficiently high $M_w > M_e$, lead to a widening of the interfacial zone sufficient to promote good mechanical strength. The good adhesion exhibited by these blends is observed despite the fact that the PS(33K) is not 'wetted' by the PS(105K) phase owing to the unfavourable entropic factor. Thus, the good mechanical strength is attributable to a

sufficiently high M_w for all blend components, and to the net effect of the attraction between the SAN and PMMA(32K) and the repulsion between the SAN and the PS(33K) block, which widen the interfacial region, inducing intermolecular adhesion and mechanical coupling (entanglement) between them.

SAN/B(20K)/PS(17K)

The B(20K) block copolymer has PS(10K) and PMMA(10K) block segments. The mechanical behaviour of these blends appears to result from the comparative level of the adhesive strength between the block copolymer and the matrix polymers and the cohesive strength within the polystyrene matrix, i.e. PS(17K)-

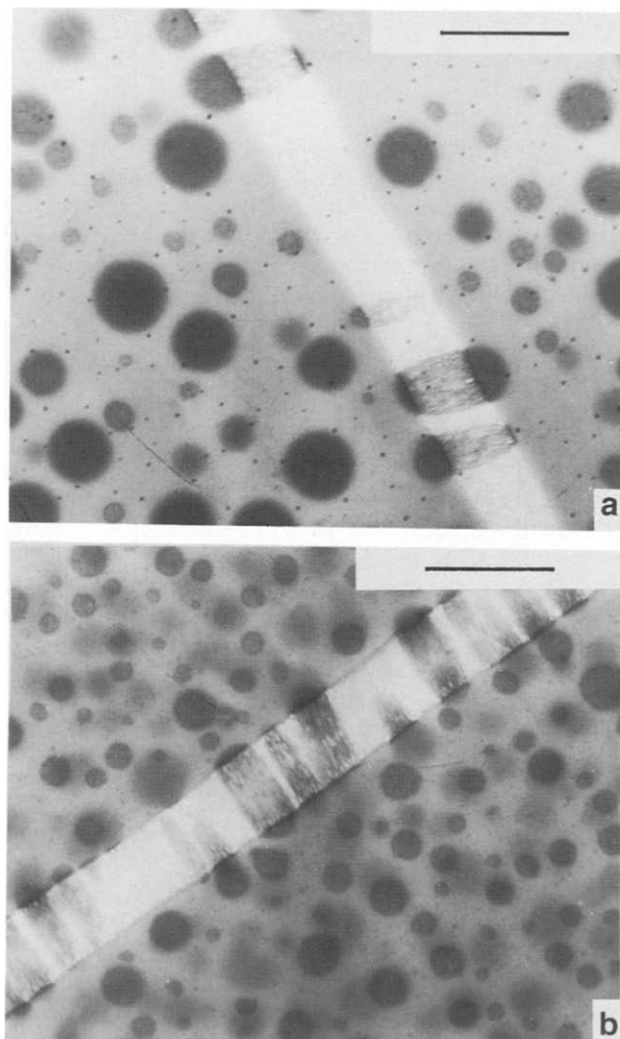


Figure 9 Deformed PS spheres in (a) PMMA/PS(105K) and (b) PMMA/B(20K)/PS(105K). No differences in interfacial strength are visible, although the emulsifying power of the block copolymer is evident in the smaller disperse phase sizes in (b). Scale bars are 2 μm

Table 2 Interaction energies between SAN/PMMA and SAN/PS

Matrix	$B_{\text{SAN-MMA}}$ (cal cm^{-3})	$B_{\text{SAN-S}}$ (cal cm^{-3})
SAN15	-0.0890	1.011
SAN26	-0.0940	1.752
SAN29	-0.0674	1.955
SAN33	-0.0126	2.224

PS(17K) interaction. Broken PS(17K) spherical domains were observed in the deformation zones (Figures 4a–d), showing that the adhesive strength of the block with the matrix (PS(10K)–PS(17K)) is higher than the cohesive effect of PS(17K)–PS(17K). Again, the block copolymer–matrix strength can be rationalized to have resulted from the net effect of the repulsion of the PS(10K) by the SAN matrix and the attraction between the PMMA(10K) and the SAN, which increases interfacial width and promotes good adhesion. Unfortunately, because of the weak cohesive strength of the PS(17K) matrix, no discrimination on the basis of varying degrees of enthalpic interaction is possible.

SAN/B(20K)/PS(105K)

Entropy-driven swelling of the blocks (PS(10K) and PMMA(10K)) by the SAN and PS(105K) matrices is clearly absent. Also, the PS block length is insufficient to form mechanical entanglements, while the PMMA segment length is comparable to M_e . Since the block copolymer molar mass is evidently close to the critical value necessary to support at least one entanglement, and there is no entropic effect, it is reasonable to expect that the interfacial strength is strongly influenced by variation in the exothermic mixing of SAN–PMMA and in the SAN–PS(10K) repulsion, each of which tends to increase the interfacial width and promote good intermolecular adhesion. Since the cohesive strength of the PS(105K) matrix is high, this system permits us to observe the influence of the enthalpic interactions on interfacial strength. The results in Figure 8 are consistent with the interpretation that the interfacial width is largest in the SAN15 blend and systematically decreases with increase in AN content. This is in agreement with earlier morphological studies³¹. In particular, attempts to stain the MMA at the interfaces in SAN/B(305K)/PS(61K) blends are only successful for SAN29 and SAN33, indicating that, for the SANs of lower AN content, the interfacial concentration of MMA is too low, i.e. the spatial extension of the MMA block is largest.

PS/PS-*b*-PMMA/PMMA

It is clear from our observations that the craze breakdown method cannot be applied to investigate interfacial reinforcement in PS/PS-*b*-PMMA/PMMA blend systems. As noted earlier, this is inferred to be due to the relatively weak repulsion between PMMA and PS. Gaines³⁵ showed that the interfacial tension in PS/PMMA blends is relatively small. Fernandez *et al.*³⁶ used the neutron reflection technique to measure the interfacial thickness between PS and PMMA phases, and obtained a value around 20 Å. In addition, Anastasiadis and Russell³⁷ were quoted (by Brown¹⁷) to have used the same technique to obtain an interfacial thickness of 54 Å for the same system in the presence of PS–PMMA block copolymer, showing interfacial widening. As suggested by Brown¹⁷, the thickness of the interface in the neat binary blend PS/PMMA (20 Å) may be sufficient for a strong entanglement interaction between the PS and PMMA chains. Barlow and Paul⁴ have argued that there is an appreciable interfacial strength between PMMA and PS in lap shear tests. We carried out morphological studies on PS/PMMA cast from MEK solution, dried and annealed in vacuum at 100°C for 2 and 7 days, which show that there is no morphologically

distinguishable interfacial behaviour between the two samples. Therefore, the interfacial strength in the neat blend is not attributable to the presence of residual solvent at the interface. We, therefore, conclude that the interface in neat PS/PMMA is indeed wide enough for the chains to form mechanically effective entanglements. No differences in the mechanical behaviour of the interfaces of PS/PMMA blends either with or without block copolymers were discernible when block copolymers PS-*b*-PMMA of molar masses of 20 000, 65 000 and 680 000 g mol⁻¹ were added (see Figures 9a and 9b).

CONCLUSIONS

Enthalpic effects on interfacial adhesion in SAN/PS blends reinforced with PS-*b*-PMMA block copolymers have been isolated and studied. Statistical analysis and the visual observations of interfacial failure of PS inclusions within crazes in the binary and ternary blends lead to the following conclusions.

Entropic and enthalpic effects on interfacial adhesion cannot be distinguished when the molar masses of the block copolymer segments and the matrix polymers are substantially higher than the entanglement molar mass, M_e .

In the SAN/B(20K)/PS(17K) blends, the observation of fractured PS(17K) spheres shows that the interfacial interpenetration that results from the addition of B(20K) is large enough for mechanical reinforcement.

In the SAN/B(20K)/PS(105K) blends, we find increasing interfacial failure with AN content, indicating that the effectiveness of interfacial interpenetration decreases owing to a systematic change in the net enthalpic interaction.

The minimum copolymer block length necessary for interfacial reinforcement and hence the effectiveness of entanglement coupling across the interface is influenced by the balance in short-range (attractive and repulsive) interactions between the blend components.

The inability to distinguish visually between the interfacial adhesion of the neat PMMA/PS and the ternary PMMS/B/PS blends illustrates that the craze breakdown approach is limited to immiscible blends that have comparatively narrow interfaces.

ACKNOWLEDGEMENTS

This work was made possible by a graduate fellowship to A. Adedeji from the Goodyear Tire and Rubber Co. and by financial support from the Edison Polymer Innovation Corp.

REFERENCES

- 1 Olabisi, P., Robeson, L. M. and Shaw, M. T. 'Polymer–Polymer Miscibility', Academic Press, New York, 1979
- 2 Paul, D. R. and Newman, S. (Eds.) 'Polymer Blends', Academic Press, New York, 1978, Vol. 1, Ch. 6
- 3 Helfand, E. and Tagami, Y. *J. Chem. Phys.* 1972, **56**, 3592
- 4 Barlow, J. W. and Paul, D. R. *Polym. Eng. Sci.* 1984, **24**, 525
- 5 Creton, C., Kramer, E. J. and Hadziioannou, G. *Macromolecules* 1991, **24**, 1846
- 6 Paul, D. R. and Barlow, J. W. *J. Macromol. Sci., Rev. Macromol. Chem. (C)* 1980, **18**, 109
- 7 Xanthos, M. *Polym. Eng. Sci.* 1988, **28**, 1392
- 8 Brown, H. R. *Macromolecules* 1991, **24**, 2752
- 9 Noolandi, J. and Hong, K. M. *Macromolecules* 1982, **15**, 482

- 10 Noolandi, J. and Hong, K. M. *Macromolecules* 1984, **17**, 1531
- 11 Coleman, M. M., Graf, J. F. and Painter, P. C. 'Specific Interactions and Miscibility of Polymer Blends', Technomic, Basel, 1991, Ch. 2, p. 113
- 12 Yeung, C., Balazs, A. C. and David, J. *Macromolecules* 1992, **25**, 1357
- 13 Shull, K. R. and Kramer, E. J. *Macromolecules* 1990, **23**, 4769
- 14 Leibler, L. *Makromol. Chem., Macromol. Symp.* 1988, **16**, 1
- 15 Vilgis, T. A. and Noolandi, J. *Macromolecules* 1990, **23**, 2941
- 16 Vilgis, T. A. and Noolandi, J. *Makromol. Chem., Macromol. Symp.* 1988, **16**, 225
- 17 Brown, H. R. *Macromolecules* 1989, **22**, 2859
- 18 Brown, H. R. *Nature* 1989, **341**, 221
- 19 Kausch, H. H. 'Polymer Fracture', 2nd Edn, Springer, Berlin, 1987
- 20 Brown, H. R., Char, K. and Deline, V. R. *Macromolecules* 1990, **23**, 3383
- 21 Sauer, J. A. and Hara, M. *Adv. Polym. Sci.* 1990, **91** (2), 85
- 22 Wellinghoff, S. T. and Baer, E. *J. Polym. Sci., Polym. Phys. Edn.* 1985, **20**, 1129
- 23 Moon, P. C. and Barker, R. E., Jr *J. Polym. Sci., Polym. Phys. Edn.* 1973, **11**, 909
- 24 Yang, A. C. M., Kramer, E. J., Kuo, C. C. and Phoenix, S. L. *Macromolecules* 1986, **19**, 2020
- 25 Moore, R. S. and Gieniewski, C. *J. Appl. Polym. Sci.* 1970, **14**, 2889
- 26 Kramer, E. J. and Berger, L. L. *Adv. Polym. Sci.* 1990, **91/92**, 1
- 27 Berger, L. L. *Macromolecules* 1990, **23**, 2926
- 28 Quintens, D. and Groeninckx, G. *Polym. Eng. Sci.* 1991, **31**, 1215
- 29 Fowler, M. E., Barlow J. W. and Paul, D. R. *Polymer* 1987, **28**, 1177
- 30 Fowler, M. E., Barlow, J. W. and Paul, D. R. *Polymer* 1987, **28**, 2145
- 31 Akiyama, M. and Jamieson, A. M. *Polymer* 1992, **33**, 3582
- 32 Ferry, J. D. 'Viscoelastic Properties of Solid Polymers', 3rd Edn., Wiley, New York, 1980
- 33 Thomas, E. L. and Winey, K. I. *Proc. ACS Div. Polym. Mater. Sci. Eng.* 1990, **62**, 686
- 34 Fayt, R., Jerome, R. and Teyssie, Ph. *Polym. Eng. Sci.* 1987, **27**, 328
- 35 Gaines, G. L. *Polym. Eng. Sci.* 1972, **12**, 1
- 36 Fernandez, M. L., Higgins, J. S., Penfold, J., Ward, R. C., Shakleton, C. and Walsh, D. J. *Polymer* 1988, **29**, 1923
- 37 Anastasiadis, S. H. and Russell, T. P. unpublished results
- 38 Plummer, C. J. G. and Donald, A. M. *Macromolecules* 1990, **23**, 3929